"Brain age" relates to early life factors but not to accelerated brain aging

Vidal-Piñeiro, D. PhD[1]*, Wang, Y. PhD[1], Krogsrud, SK. PhD[1], Amlien, IK. PhD[1], Baaré, WFC. PhD[2], Bartrés-Faz, D. PhD[3], Bertram, L. MD[1,4], Brandmaier, A.M. Dr[5,6], Drevon CA. MD, PhD[7], Düzel, S. PhD[6], Ebmeier KP., MD[8], Henson RN PhD[9], Junque, C. PhD[3,10], Kievit RA[9,11], Kühn, S. PhD[12,13], Leonardsen, E. MsC[1], Lindenberger, U. PhD[5,6], Madsen, KS. PhD[2,14], Magnussen, F. MsC[1], Mowinckel, AM. PhD[1], Nyberg, L. PhD[15], Roe, JM. PhD[1], Segura B. PhD[3,10], Sørensen, Ø. PhD[1], Suri S. DPhil[16], Zsoldos E. DPhil[16], the Australian Imaging Biomarkers and Lifestyle flagship study of ageing**, Walhovd, KB. PhD[1,17], and Fjell, AM. PhD[1,17]

[1]Centre for Lifespan Changes in Brain and Cognition, Department of Psychology, University of Oslo, Oslo, Norway.

[2]Danish Research Centre for Magnetic Resonance, Centre for Functional and Diagnostic Imaging and Research, Copenhagen University Hospital Hvidovre, Hvidovre, Denmark

[3]Department of Medicine, Faculty of Medicine and Health Sciences, Institute of Neurosciences, University of Barcelona; Institute of Biomedical Research August Pi i Sunyer (IDIBAPS), Barcelona, Spain

[4]Lübeck Interdisciplinary Platform for Genome Analytics (LIGA), Institutes of Neurogenetics and Cardiogenetics, University of Lübeck, Lübeck, Germany

[5]Max Planck UCL Centre for Computational Psychiatry and Ageing Research, Berlin, Germany

[6]Center for Lifespan Psychology, Max Planck Institute for Human Development, Berlin, Germany

[7]Department of Nutrition, Inst Basic Med Sciences, Faculty of Medicine, University of Oslo & Vitas Ltd, Science Park, Oslo, Norway

[8]Department of Psychiatry, University of Oxford, Oxford, UK.

[9]MRC Cognition and Brain Sciences Unit, University of Cambridge, Cambridge, UK

[10]Centro de Investigación Biomédica en Red sobre Enfermedades Neurodegenerativas (CIBERNED), Barcelona, Spain.

[11]Cognitive Neuroscience Department, Donders Institute for Brain, Cognition and Behavior, Radboud University Medical Center, Nijmegen, The Netherlands

[12]Lise Meitner Group for Environmental Neuroscience, Max Planck Institute for Human Development, Berlin, Germany

[13]Department of Psychiatry, University Medical Center Hamburg-Eppendorf, Germany

[14]Radiography, Department of Technology, University College Copenhagen, Copenhagen, Denmark

[15]Umeå Centre for Functional Brain Imaging, Umeå, Sweden; Department of Integrative Medical Biology, Physiology Section and Department of Radiation Sciences, Diagnostic Radiology, Umeå University, Umeå, Sweden.

[16]Wellcome Centre for Integrative Neuroimaging, Departments of Psychiatry and Clinical Neuroscience, University of Oxford, Oxford, UK.

[17]Department of radiology and nuclear medicine, Oslo University Hospital, Oslo, Norway.

**Some of the data used in the preparation of this article were obtained from the Australian Imaging Biomarkers and Lifestyle flagship study of ageing (AIBL) funded by the Commonwealth Scientific and Industrial Research Organisation (CSIRO), which were made available at the ADNI database (www.loni.usc.edu/ADNI). The AIBL researchers contributed data but did not participate in the analysis or writing of this report. AIBL researchers are listed at www.aibl.csiro.au.

Corresponding author:

Didac Vidal Piñeiro

Department of Psychology, Pb. 1094 Blindern

Oslo, Norway, 0317

d.v.pineiro@psykologi.uio.no

Tel: (+47) -22845061

Running title: Brain age unrelated to aging

Abstract

Brain age is an influential index for quantifying brain health, assumed partially to reflect the rate of brain aging. We explicitly tested this assumption in two large datasets and found no association between cross-sectional *brain age* and steeper brain decline. Rather, *brain age* in adulthood was associated with early-life influences indexed by birth weight and polygenic scores. The results call for nuanced interpretations of cross-sectional indices of the aging brain.

Keywords

Aging, Brain age gap, Brain age delta, BrainAGE, PAD, neuroimaging, brain decline, T1w

Introduction

The concept of *brain age* is increasingly used to capture inter-individual differences in the integrity of the aging brain[1]. The biological age of the brain is estimated typically by applying machine learning to magnetic resonance imaging (MRI) data to predict chronological age. The difference between *brain age* and chronological age (*brain age delta*) reflects the deviation from the expected norm and is often used to index brain health. *Brain age delta* has been related to brain, mental, and cognitive health and proved valuable in predicting outcomes such as mortality[1–3]. To different degrees, it is assumed that *brain age delta* reflects past and ongoing neurobiological aging processes[1,3–6]. Hence, it is common to interpret positive *brain age deltas* as reflecting accelerated aging[1,4,6].

The assumption that *brain age delta* reflects an ongoing process of neurobiological aging implies that there should be a relationship between cross-sectional and longitudinal estimates of *brain age*. Alternatively, deviation from the expected *brain age* could show lifelong stability and capture early genetic and environmental influences[3,7,8]. These perspectives offer fundamentally divergent interpretations of results showing higher *brain age (delta)* in groups experiencing specific life events, brain disorders, and other medical problems. Here we tested whether *brain age* is related to accelerated brain aging, early-life factors, or a combination of both (**Fig. 1a**). If *brain age* reflects accelerated brain aging, cross-sectional *brain age delta* - indexed by the centercept - should be positively associated with yearly increases of *brain age delta* over time *(brain age delta$_{long}$).* If the early-life account plays a substantial role, one should observe a relationship between *brain age* and early factors - indexed here as birth weight and polygenic scores for *brain age* (PGS-BA) given evidence of lifelong effects of genetic risk on age-related phenotypes[9,10] (**Fig. 1b**).

Results

Chronological age (**Fig. 1c**) was predicted based on multimodal regional and global features from structural T1-weighted (T1w) MRI, including cortical thickness, area, volume, and gray-white matter contrast, as well as volume and intensity of subcortical structures (|N| = 365). See list in **Supplementary Table 1, 2,** and **Fig. 1d** for pairwise correlations with age. The model was trained on 38682 participants with a single MRI from the UK Biobank[11] dataset using gradient boosting as implemented in XGBoost (https://xgboost.readthedocs.io) and optimized using 10-fold cross-validation and a randomized hyper-parameters search. The trained model (**Fig. 1e**) was then used to predict *brain age* for an independent test dataset of 1372 participants with 2 MRIs each (age range = 47.2 - 80.6 years, mean [SD] follow-up = 2.3 [0.1] years). The predictions revealed a high correlation between chronological and *brain age* (r = 0.82) with mean absolute error (MAE) = 3.31 years and root mean squared error (RMSE) = 4.14 years (**Fig. 1f**), comparable to other *brain age* models using UK Biobank MRI data[12]. *Brain age delta* was calculated as the difference between brain and chronological age. We used generalized additive models (GAM) to correct for the brain-age bias, i.e., the *underestimation* of brain age in older individuals and vice versa[6]. *Brain age delta* at baseline and follow-up were strongly correlated (r = 0.81). To corroborate generalizability, we replicated our results using a different machine learning algorithm – a LASSO-based approach[12] - and an independent longitudinal sample from the Lifebrain consortium[13] with up to 11.2 years of follow-up (3292 unique participants, age range = 18.0 - 94.4 years). See **Supplementary Fig. 1** and **Supplementary Table 3** for additional information. All the code used to generate the results will be available at https://github.com/LCBC-UiO/VidalPineiro_BrainAge.

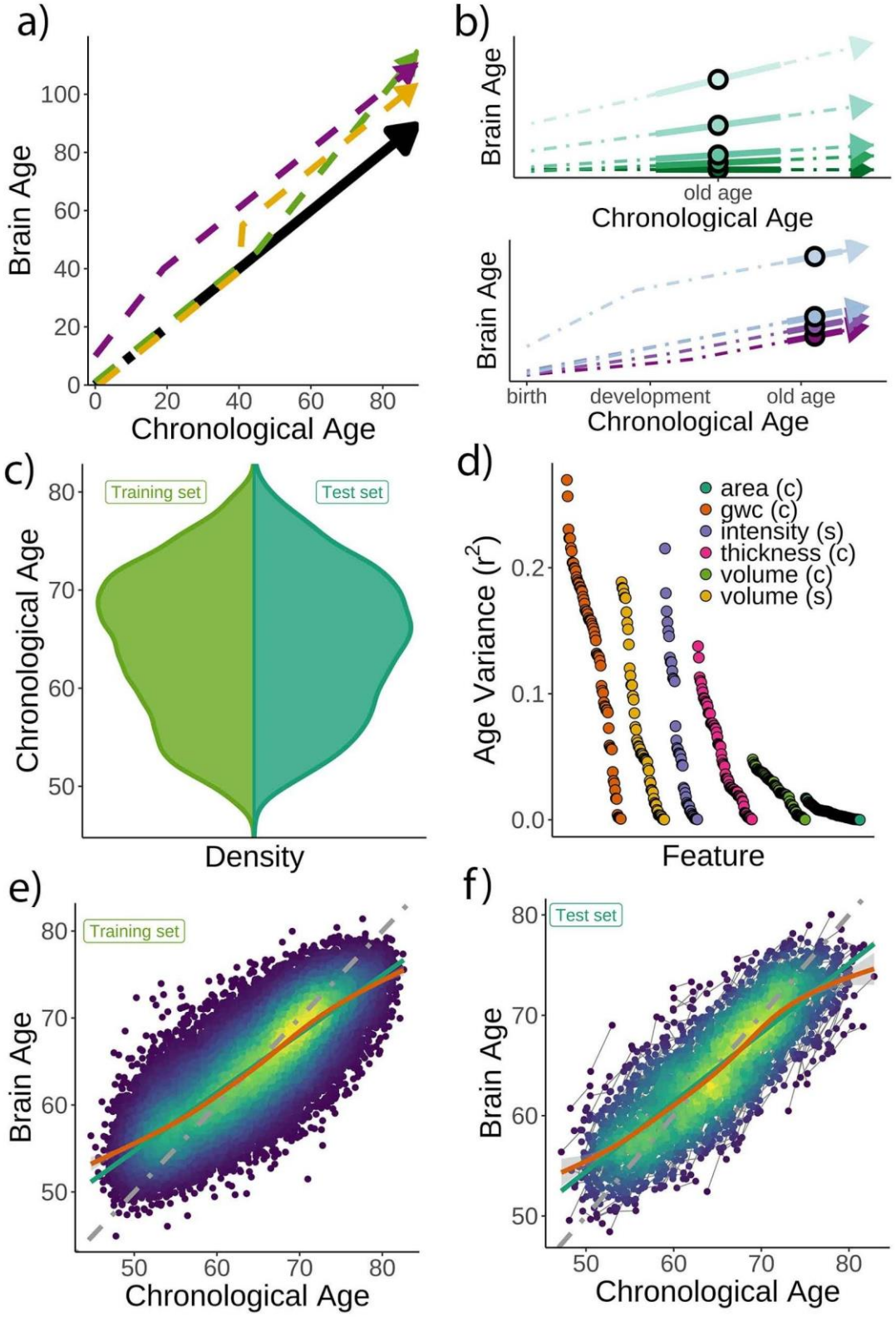

Fig. 1. Theoretical expectations and study characteristics. a) Three hypothetical trajectories leading to higher *brain age delta*. Higher *brain age delta* can be explained by a steeper rate of neurobiological aging (green), distinct events that led to the accumulation of brain damage in the past (yellow), or early-life genetic and developmental factors (purple). The black

arrow represents normative values of *brain age* through the lifespan. **b)** Brain aging (green) vs. early-life (blue-purple) accounts of *brain age* in older age. For the brain aging notion, cross-sectional *brain age* (points) relates to the slope of *brain age* as assessed by two or more observations across time (continuous line), reflecting ongoing differences in the rate of aging (dashed line, green scale). For the early-life notion, cross-sectional *brain age* (points), relates to early environmental, genetic, and/or developmental differences such as birth weight (blue-purple scale). **c)** Relative age distribution for the UK Biobank test and training datasets. **d)** Age variance explained (r^2) for each MRI feature in the training dataset. Features are grouped by modality and ordered by the variance explained. **e)** *Brain age* model as estimated on the training (n = 38682), and **f)** test datasets (participants = 1372; two observations each). In **e)** and **f)**, lines represent the identity (grey), the linear (green), and the GAM (orange) fits of *brain age* by chronological age. Confidence intervals represent standard errors (SE). In **d)** gwc = gray-white matter contrast, (c) = cortical, and (s) = subcortical.

First, we tested whether cross-sectional *brain age delta* predicted *brain age delta*$_{long}$ using linear models controlling for age, sex, site, and estimated intracranial volume (eICV). We selected the centercept (mean), instead of baseline *brain age delta*, to avoid statistical dependency between indices. We found a weak significant negative relation between cross-sectional and *brain age delta*$_{long}$ in the UK Biobank (β = -0.016 [± 0.008] year/*delta*, t (p) = -2.0 (.04), r^2 = .002, **Fig. 2a**). Cross-sectional and *brain age delta*$_{long}$ were unrelated using a LASSO regression approach (β = -0.003 [± 0.006] year/*delta*, t (p) = -0.5 (.65), r^2 = .0001, **Fig. 2b**), and in the Lifebrain replication sample (β = -0.007 [± 0.01] year/*delta*, t (p) = -0.6 (.53), r^2 = .0001, **Fig. 2c**). Post-hoc equivalence tests showed that positive relationships larger than β = 0.01 year/*delta* would be rejected in all three analyses thus confirming a lack of a meaningful relationship between cross-sectional and longitudinal *brain age* (**Methods** and **Supplementary Fig. 2**). Lifebrain results remained unaffected after restricting the analysis to participants with long follow-up intervals (>4 years). See **Methods** and **Supplementary Fig. 3** for details.

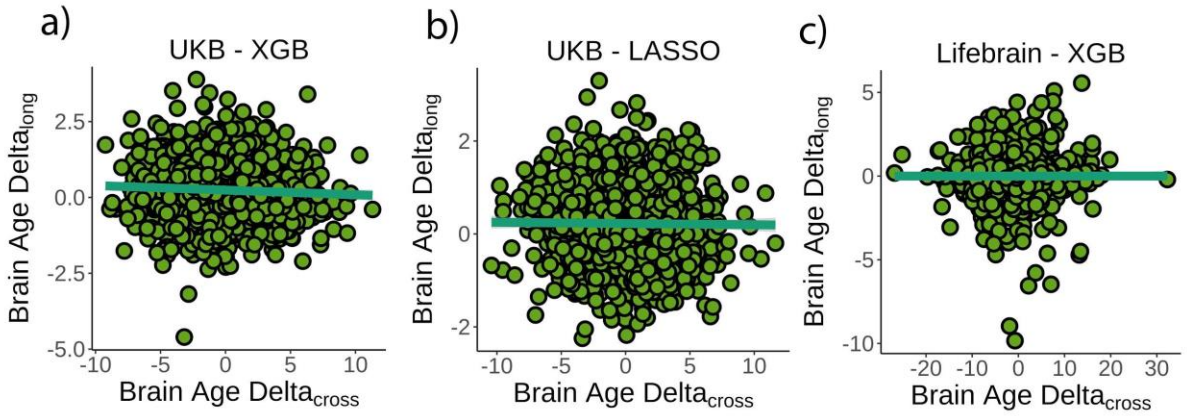

Fig. 2. Relationship between cross-sectional and longitudinal *brain age delta*. a) Main analysis using the UK Biobank dataset and boosting gradient (n = 1372). **b)** Replication analyses using a different training algorithm (LASSO; n = 1372) and **c)** an independent dataset (Lifebrain; n = 1500). XGB = boosting gradient as implemented in XGBoost. Confidence intervals represent SE.

Next, we tested if birth weight was associated with *brain age delta* or change in *brain age delta*. Linear mixed models were used to fit time (from baseline; years), birth weight, and its interaction on *brain age delta*, using age at baseline, sex, site, and eICV as covariates. Birth weight was significantly related to *brain age delta* (β = -0.70 [± .30] year/kg, t (p) = -2.3 (.02), r^2 = .009, **Fig. 3a**) but not to *delta* change (β = 0.02 [± .09] year/kg, t (p) = 0.3 (.79)). Birth weights were limited to normal variations at full-term (from 2.5 to 4.5 kg) (n = 770 unique individuals) but see **Supplementary Fig. 4** for results with varying cut-offs. The results were not affected by excluding individuals born in multiple births (p = .02) and were replicated using the LASSO approach (β = -0.79 [± .29] year/kg, t (p) = -2.8 (0.006), r^2 = .009, **Fig. 3b).**

Finally, we tested whether polygenic scores for *brain age delta* (PGS-BA) related to *brain age delta* and change in *brain age delta* (n = 1339). PGS-BA was computed using a mixture-normal model based on a genome-wide association study (GWAS) of the *brain age delta* phenotype in the UK Biobank training dataset. To test the association, linear mixed models were used as above with 10 additional

covariates accounting for population structure. See **Supplementary Fig. 5** for GWAS results. PGS-BA was positively associated with *brain age delta* (β = 0.54 [± 0.09] year/kg, t (p) = 9.4 (< .001), r^2 = .02, **Fig. 3c)** and negatively associated with *brain age delta* change (β = -0.06 [± .03] year/kg, t (p) = -2.4 (0.02)) in the independent test dataset**.** Likewise, PGS-BA was associated with *brain age delta* derived from the LASSO algorithm (β = 0.53 [± 0.09] year, t (p) = 10.4 (< 0.001), r^2 = .02) but not to *brain age delta* change (β = -0.001 [± .02] year, t (p) = 0.0 (1.0)).

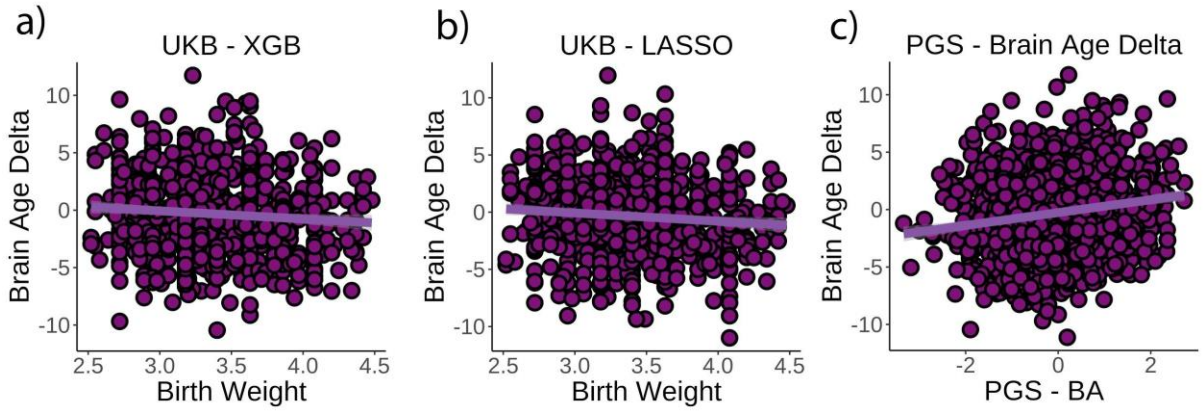

Fig. 3. Relationship between cross-sectional *brain age delta and birth weight*. a) Main analysis using the UK Biobank dataset and boosting gradient (n = 770). **b)** Replication analyses using a different training algorithm (LASSO) (n = 770). **c)** Relationship between polygenic scores for *brain age delta* and *brain age delta* (n = 1339). XGB = boosting gradient as implemented in XGBoost. Confidence intervals represent SE.

Discussion

Altogether, these findings do not support the claim that cross-sectional *brain age* is related to ongoing brain aging. Rather, *brain age* seems to reflect early-life influences, and only to a negligible degree actual brain change in middle and old adulthood. A lack of relationship between *brain age* and rate of brain aging can potentially be explained by the effect of circumscribed events such as isolated insults or detrimental lifestyles that occurred in the past resulting in higher but not accelerating, *brain age*. Yet, variations in *brain age* can equally reflect developmental and early-life differences and show lifelong stability. *Brain-age* paradigms are generally ill-suited for disentangling between these sources of variation but are often interpreted in line with the former. This assumes that variation in *brain age* largely results from the accumulation of damage and insults during the lifespan, with similar starting points for everyone. An exception is Elliott and colleagues[3], who found that middle-aged individuals with higher brain age already exhibited poorer cognitive function and brain health at age three years. This fits a robust corpus of literature showing effects of lifelong, stable influences as indexed by childhood IQ[14], genetics[10], and neonatal characteristics[8] on brain and cognitive variation in old age.

Strictly speaking, *brain age delta* is a prediction error from a model that maximizes the prediction of age in cross-sectional data. Prediction errors also reflect noise, attenuating any relation between cross-sectional and longitudinal *brain age*. The Lifebrain replication sample with more observations and longer follow-up reduces the likelihood of noise as the main factor behind the lack of relationship. Furthermore, previous studies have found that changes in *brain age* are partly heritable[15], suggesting that it captures biologically relevant signal, although with substantially different origins from cross-sectional *brain age*. Without longitudinal imaging, one should thus not interpret brain age as accelerated aging. This aligns with theoretical claims and empirical observations that covariance structures capturing differences between individuals do not necessarily generalize to covariance

structures within individuals[16,17]. Neither does indirect evidence, via associations with other bodily markers of aging or with cognitive decline, yield decisive support for cross-sectional *brain age* as a marker of individual differences in brain aging[2,3,18]. Relationships between cross-sectional and longitudinal *brain age* may thus be restricted to specific disease groups such as Alzheimer's disease patients[18] where interindividual brain variation is dominated by the prevailing loss of brain structural integrity.

The results further showed that birth weight, which reflects differences in genetic propensities and to a large degree prenatal environment[19], explained a modest portion of the variance in *brain age*. Subtle variations in birth weight are associated with brain structure early in life and present throughout the lifespan[8]. This association should be considered as *proof-of-concept* that the metric of *brain age* reflects the distant past more than presently ongoing events in the morphological structure of the brain. This was confirmed by the consistent association between PGS-BA and *brain age delta* but not with *brain age delta* change. Since PGS-BA was computed based on cross-sectional *brain age delta*, this relationship may not be surprising, but still suggests a different genetic foundation for longitudinal *brain age*. These findings link with evidence that brain development is strongly influenced by genetic architecture that, in interaction with environmental factors, lead to substantial, long-lasting effects on brain structure. By contrast, aging mechanisms seem to be more related to limitations of maintenance and repair functions and have a more stochastic nature[20].

As distance from birth increases, chronological age as a marker of individual development is reduced. The results call for caution in interpreting brain-derived indices of aging based on cross-sectional MRI data and underscores the need to rely on longitudinal data whenever the goal is to understand the trajectories of brain and cognition in aging.

Methods

Participants and Samples

The main sample was drawn from the UK Biobank neuroimaging branch (https://www.ukbiobank.ac.uk/)[11]. 38682 individuals had MRI available at a single time point and were used as the training dataset. 1372 individuals had longitudinal data and were used as the test dataset. The present analyses were conducted under data application number 32048. The Lifebrain dataset[13] included datasets from 5 different major European Lifespan cohorts: the Center for Lifespan Changes in Brain and Cognition cohort (LCBC, Oslo)[8], the Cambridge Center for Aging and Neuroscience study (Cam-CAN)[21,22], the Berlin Study of Aging-II (Base-II)[23], the University of Barcelona cohort (UB)[24,25], and the BETULA project (Umeå)[26]. Furthermore, we included data from the Australian Imaging Biomarkers and Lifestyle flagship study of ageing (AIBL)[27]. In addition to cohort-specific inclusion and exclusion criteria, individuals aged < 18 years, or with evidence of mild cognitive impairment, or Alzheimer's Disease were excluded from the analyses. 1792 individuals with only one available scan were used for the Lifebrain training dataset. 1500 individuals with available follow-up of > 0.4 years were included in the test dataset. Individuals had between 2 and 8 available scans each. Sample demographics for the UK Biobank and the Lifebrain samples are provided in **Supplementary Table 3**. See also **Fig. 1c** and **Supplementary Fig. 1** for a visual representation of the age distribution in the UK Biobank and the Lifebrain datasets. UK Biobank (North West Multi-Center Research Ethics Commitee [MREC]; see also https://www.ukbiobank.ac.uk/the-ethics-and-governance-council) and the different cohorts of the Lifebrain replication dataset (**Supplementary Table 4**) have ethical approval from the respective regional ethics committees . All participants provided informed consent.

MRI acquisition and preprocessing

See https://biobank.ctsu.ox.ac.uk/crystal/crystal/docs/brain_mri.pdf for details on the UK Biobank T1-weighted (T1w) MRI acquisition. UK Biobank and Lifebrain MRI data were acquired with 3 and 10

different scanners, respectively. T1w MRI acquisition parameters for both the Lifebrain and the UK Biobank are summarized in **Supplementary Table 5**.

We used summary regional and global metrics derived from T1w data. For UK Biobank we used the imaging-derived phenotypes developed centrally by UK Biobank researchers[11] and distributed via the data showcase (http://biobank.ctsu.ox.ac.uk/crystal/index.cgi). See preprocessing details in https://biobank.ctsu.ox.ac.uk/crystal/crystal/docs/brain_mri.pdf. This procedure yielded 365 structural MRI features, partitioned in 68 features of cortical thickness, area, and gray-white matter contrast, 66 features of cortical volume, 41 features of subcortical intensity, and 54 features of subcortical volume. See the list of features in **Supplementary Table 1** and **2**. Lifebrain data were processed on the Colossus processing cluster, University of Oslo. Similar to the UK Biobank pipeline, we used the fully automated longitudinal FreeSurfer v.6.0. pipeline[28] for cortical reconstruction and subcortical segmentation of the structural T1w data (http://surfer.nmr.mgh.harvard.edu/fswiki)[29–31] and used similar atlases for structural segmentation and feature extraction.

Birth weight

We used birth weight (Kg) from the UK Biobank (*field #20022*). Participants were asked to enter their birth weight at the initial assessment visit, the first repeat assessment visit, or the first imaging visit. In the case of multiple birth weight instances, we used the latest available input. n = 894 participants from the test dataset had available data on birth weight. The main analysis was constrained to normal variations in birth weight between 2.5 and 4.5 Kg (n = 770)[32] due to lower reliability of extreme scores and to tentatively remove participants with severe medical complications associated with prematurity.

Genetic preprocessing

Detailed information on genotyping, imputation, and quality control was published by Bycroft and colleagues[33]. For genetic analyses, we only included participants with both genotypes and MRI scans. Following the recommendations from the UK Biobank website, we excluded individuals with failed genotyping, that had abnormal heterozygosity status, or that withdrew their consents. We also removed participants that were genetically related – up to the third degree – to at least another participant as estimated by the kinship coefficients as implemented in PLINK[34]. For the genome-wide association study (GWAS) we used 38163 individuals from the training dataset. Polygenic risk scores were computed to the test dataset consisting of 1339 individuals with longitudinal MRI.

GWAS

We performed GWAS analysis on the training dataset and the *brain age delta*-corrected phenotype (based on a generalized additive model [GAM]) fit. To control for possible effects in the structure of the population, we computed the top 10 principal components (PCs) using the PLINK command *–pca* on a decorrelated set of autosome single nucleotide polymorphisms (SNPs). The set of SNPs (n=101797) were generated by using the PLINK command, *--maf 0.05*, *--hwe 1e^{-6}, --indep-pairwise 100 50 0.1*. The *–glm* function was used to perform GWAS including age, sex, and the top 10 PCs as covariates. See Manhattan and quantile-quantile (QQ) plots in **Supplementary Fig. 5**. Note that results show a similar profile as in Jonsson and colleagues[35].

Polygenic scores (PGS)

The GWAS results for the training dataset were used to compute PGS (PGS-BA) in the independent test dataset (n = 1339 participants). We used the recently developed method PRS-CS[36] to estimate the posterior effect sizes of SNPs that were shown to have high quality in the HapMap data[37]. Rather than estimating the polygenicity of *brain age delta* from our data, we assumed a highly polygenic

architecture for *brain age delta* by setting the parameter *--phi=0.01*[38]. The remaining parameters of PRS-CR were set to the default values. PGS was based on 654725 SNPs and was computed on the independent test data using the *--score* function from PLINK. We also computed the population structures PCs' in the test dataset using the same procedure as in the training dataset.

Statistical analyses

The code used in this manuscript is available at https://github.com/LCBC-UiO/VidalPineiro_BrainAge. All statistical analyses were run with R version 3.6.3 https://www.r-project.org/. We used the UK Biobank as the main sample and the Lifebrain cohort for independent replication. The main description refers to the UK Biobank pipeline, though Lifebrain replication followed identical steps unless otherwise stated. For replication across machine learning pipelines, we used a LASSO regression approach for age prediction, adapted from https://james-cole.github.io/UKBiobank-Brain-Age/. See more details in Cole, 2020[12]. The correlation between LASSO-based and Gradient Boosting-based *brain age deltas* was .80.

Brain age prediction

We used machine learning to estimate each individuals' *brain age* based on a set of regional and global features extracted from T1w sequences. We estimated *brain age* using gradient tree boosting (https://xgboost.readthedocs.io). We used participants with only one MRI scan for the training dataset (n = 36682) and participants with longitudinal data as test dataset (n = 1372). All variables were scaled prior to any analyses using the training dataset metrics as reference.

The model was optimized in the training set using a 10-fold cross-validation randomized hyper-parameters search (50 iterations). The hyper-parameters explored were number of estimators [100, 600, 50], learning rate (0.01, 0.05, 0.1, 0.15, 0.2), maximum depth [2, 8, 1], gamma regularisation

parameter [0.5, 1.5, 0.5], and min child weight [1, 4, 1]. The remaining parameters were left to default. The optimal parameters were: number of estimators = 500, learning rate = 0.1, maximum depth = 5, gamma = 1, and min child weight = 4 predicting r^2 = 0.68 variance in chronological age with mean absolute error (MAE) = 3.41 and root mean squared error (RMSE) = 4.29. See visual representation in **Fig. 1f**.

Next, we recomputed the machine learning model using the entire training dataset and the optimal hyper-parameters and used it to predict *brain age* for the test dataset. The predictions revealed a high correlation between chronological and brain-predicted age (r = 0.82) with MAE = 3.31 years and RMSE = 4.14 years (**Fig. 1e)**. These metrics are similar or better than other *brain age* models using UK Biobank MRI data[12,39], and than the cross-validation diagnostics. *Brain age delta* was estimated as the difference between *brain age* and chronological age. We used GAM to correct for the brain-age bias estimation where *brain age* is underestimated in older ages[6]; r = -0.54 for the test dataset. Note that we used GAM fittings as estimated in the training dataset so *delta* values in the test dataset are not centered to 0. The correlation between *brain age delta* corrected based on the training vs. the test fit was r > 0.99. Also, GAM-based bias correction led to similar brain age delta estimations to linear and quadratic-based corrections (r > 0.99).

Higher level-analysis

Relationship between cross-sectional and longitudinal brain age. For each participant, we computed the mean *brain age delta* across the two MRI time points and the yearly rate of change (*brain age* $delta_{long}$). We selected mean, instead of baseline *brain age delta*, to avoid statistical dependency between both indices[40,41]. *Brain age* $delta_{long}$ was fitted by mean *brain age delta* using a linear

regression model, which accounted for age, sex, site, and estimated intracranial volume (eICV). We used mean eICV across both time points.

Relationship between brain age PGS and cross-sectional and longitudinal brain age. This association was tested using linear mixed models with time from baseline (years), PGS-BA, and its interaction on *brain age delta*. Age at baseline, sex, site, eICV, and the 10 first principal components for population structure were used as covariates. The principal components of population structure were added to minimize false positives associated with any form of relatedness within the sample. *Effects of birth weight on brain age.* Linear mixed models were used to fit time, birth weight, and its interaction on *brain age delta*, using age at baseline, sex, site, and eICV as covariates. We explored the consistency of the results by modifying the birth weight limits in a grid-like fashion [0.5, 2.7, 0.025] and [4.2, 6.5, 0.025] for minimum and maximum birth weight (**Supplementary Fig. 4**). Self-reported birth weight is a reliable estimate of actual birth weight. However, extreme values are either misestimated or reflect profound gestational abnormalities[42,43]. Assumptions were checked for the main statistical tests using plot diagnostics. Variance explained for single terms refers to unique variance (UVE), which is defined as the difference in explained variance between the full model and the model without the term of interest. For linear mixed models, UVE was estimated as implemented in the *MuMIn* r-package.

Equivalence tests. Post-hoc equivalence tests were carried to test for the absence of a relationship between cross-sectional and *brain age delta*$_{long}$[44]. Specifically, we used inferiority tests, to test whether a null hypothesis of an effect as least as large as Δ (in years/*delta*) could be rejected. We re-run the three main models assessing a relationship between cross-sectional and longitudinal *brain age delta* (UK Biobank trained with boosting gradient, UK Biobank trained with LASSO, and Lifebrain trained with boosting gradient) varying the right-hand-side test (Δ) [-0.02, 0.05, 0.001] ($p < 0.05$, one-tailed) (**Supplementary Fig. 2**).

Lifebrain-specific steps

Features. The Lifebrain cohort included |N| = 372 features. It included 8 new features compared to the UK Biobank dataset, whereas one feature was excluded (new features: left and right temporal pole area volume and thickness, cerebral white matter volume, cortex volume; excluded feature: ventricle choroid). See age-variance explained in **Supplementary Table 1** and **2** as estimated with GAMs. *Quality control.* Prior to any analysis, we tentatively removed observations for which >5% of the features fell above or below 5 SD from the sample mean. The application of this arbitrary high threshold led to the removal of 10 observations. We considered these MRI data to be extreme outliers and likely to be artifactual and/or contaminated by important sources of noise. Also, before brain prediction, we tentatively removed variance associated with the different scanners using generalized additive mixed models (GAMM) and controlling for age as a smooth factor and a subject-identifier as random intercept. This correction was performed due to differences in age distribution by scanner and lack of across scanner calibration. *Hyperparameter search and model diagnostics.* The optimal parameters for the Lifebrain replication sample were: number of estimators = 600, learning rate = 0.05, maximum depth = 4, gamma = 1.5, and min child weight = 1. Using cross-validation, the model predicted r^2 = 0.92 of the age-variance with MAE = 4.75 and RMSE = 6.31. Brain age was underestimated in older age (bias r = -0.33). *Model prediction.* The age-variance explained by *brain age* was r = 0.90 with MAE = 4.68 and RMSE = 6.06. *Brain age* was underestimated in older age (bias r = -0.25) (**Supplementary Fig. 3**). *Higher level-analysis.* For each individual, mean *brain age delta* was considered as the grand-mean *brain age delta* across the different MRI time points. To compute *brain age delta*$_{long}$ we set for each participant a linear regression model with observations equal to the number of time points that fitted *brain age delta* by time since the initial visit. Slope indexed change in *brain age delta*/year. The relationship between mean and *brain age delta*$_{long}$ was tested using linear mixed models controlling for age, sex, and eICV as fixed effects, and using a site identifier as a random intercept. Note that eICV was identical across timepoints as a result of being estimated through the longitudinal FreeSurfer pipeline.

We performed control analyses to account for possible effects of varying follow-up intervals and to consider the presence of young adults in the Lifebrain sample. We repeated the analyses including follow-up interval as an additional covariate, restricting the analysis to individuals with a follow-up of >4 years (n = 424). The relationship between cross-sectional and *brain age delta*$_{long}$ was not significant in both cases (β = -0.008 [± 0.01] year/*delta*, t (p) = -0.7 (.45); β = -0.008 [± 0.007] year/*delta*, t (p) = -1.1 (.26)). We could not obtain the required information on genetics and birth weight to replicate the analyses supporting the *early-life* account.

Data availability

The raw data were gathered from the UK Biobank, the Lifebrain cohort, and the AIBL. Raw data requests are specific to each cohort. UK Biobank and AIBL data are available upon application to UK Biobank and at https://aibl.csiro.au upon corresponding approvals. For the Lifebrain cohorts, requests for raw MRI data should be submitted to the corresponding principal investigator. See contact details in **Supplementary Table 5**. Note that MRI data availability for some individuals may be restricted as participants did not consent to share publicly their data. Different restrictions and sample agreements might be required.

Code availability

Statistical analyses in this manuscript will be available at https://github.com/LCBC-UiO/VidalPineiro_BrainAge. All analyses were performed in R 3.6.3. The scripts were run on the Colossus processing cluster, University of Oslo. UK Biobanks' data acquisition, MRI preprocessing, and feature generation pipelines are freely available (https://www.fmrib.ox.ac.uk/ukbiobank). For the Lifebrain cohorts, the image acquisition details are summarized in **Supplementary Table 4**. MRI preprocessing and feature generation scripts were performed with the freely available FreeSurfer software (https://surfer.nmr.mgh.harvard.edu/). For bash-sourcing scripts, please contact the corresponding author.

Acknowledgments

This work was supported by the Lifebrain project, funded by the EU Horizon 2020 Grant: 'Healthy minds 0–100 years: Optimising the use of European brain imaging cohorts ('Lifebrain')." Grant agreement number: 732592 (to K.B.W.). In addition, the different sub-studies are supported by different sources. LCBC: The European Research Council under grant agreements 283634, 725025 (to A.M.F.) and 313440 (to K.B.W.), as well as the Norwegian Research Council (to A.M.F., K.B.W.), the National Association for Public Health's dementia research program (A.M.F.) and the Peder Sather foundation (to D.V.P.). Betula: a scholar grant from the Knut and Alice Wallenberg (KAW) foundation to L.N. Barcelona: D.B.F. was funded by an ICREA Academia Award. D.B.F, B.S., and C.J. acknowledge the CERCA Programme/Generalitat de Catalunya and are supported by María de Maeztu Unit of Excellence (Institute of Neurosciences, University of Barcelona) MDM-2017-0729, Ministry of Science, Innovation and Universities. BASE-II has been supported by the German Federal Ministry of Education and Research under grant numbers 16SV5537/16SV5837/16SV5538/16SV5536K/01UW0808/01UW0706/01GL1716A/01GL1716B, and S.K. has received support from the European Research Council under grant agreement 677804. The Wellcome Centre for Integrative Neuroimaging is supported by core funding from award 203139/Z/16/Z from the Wellcome Trust. Drs Suri and Zsoldos were funded by an award the UK Medical Research Council (G1001354) and the HDH Wills 1965 Charitable Trust (1117747). Dr Suri is now funded by the UK Alzheimer's Society Research Fellowship (Grant Ref 441); Suri is supported by the NIHR Oxford Health Biomedical Research Centre. Data used in the preparation of this article were partially obtained from the AIBL funded by the Commonwealth Scientific and Industrial Research Organisation (CSIRO), which was made available at the ADNI database (www.loni.usc.edu/ADNI). UK Biobank is generously supported by its founding funders the Wellcome Trust and UK Medical Research Council, as well as the Department of Health, Scottish Government, the Northwest Regional

Development Agency, British Heart Foundation and Cancer Research UK. The organisation has over 150 dedicated members of staff, based in multiple locations across the UK.

Competing Interests

The authors declare no conflicts of interest.

References

1. Cole, J.H. & Franke, K. *Trends Neurosci* **40**, 681–690 (2017).
2. Cole, J.H. et al. *Molecular Psychiatry* **23**, 1385–1392 (2018).
3. Elliott, M.L. et al. *Mol Psychiatry* (2019).doi:10.1038/s41380-019-0626-7
4. Franke, K. & Gaser, C. *Front. Neurol.* **10**, (2019).
5. Smith, S.M. et al. *Elife* **9**, (2020).
6. Smith, S.M., Vidaurre, D., Alfaro-Almagro, F., Nichols, T.E. & Miller, K.L. *NeuroImage* **200**, 528–539 (2019).
7. Deary, I.J. *Gerontology* **58**, 545–553 (2012).
8. Walhovd, K.B. et al. *Proc. Natl. Acad. Sci. U.S.A.* **113**, 9357–9362 (2016).
9. Walhovd, K.B. et al. *Proc Natl Acad Sci U S A* **109**, 20089–20094 (2012).
10. Walhovd, K.B. et al. *Neurology Genetics* **6**, (2020).
11. Miller, K.L. et al. *Nat. Neurosci.* **19**, 1523–1536 (2016).
12. Cole, J.H. *Neurobiology of Aging* **92**, 34–42 (2020).
13. Walhovd, K.B. et al. *Eur. Psychiatry* **50**, 47–56 (2018).
14. Karama, S. et al. *Mol. Psychiatry* **19**, 555–559 (2014).
15. Brouwer, R.M. et al. *Cereb Cortex* doi:10.1093/cercor/bhaa296
16. Molenaar, P.C.M. *Measurement: Interdisciplinary Research and Perspectives* **2**, 201–218 (2004).
17. Schmiedek, F., Lövdén, M., von Oertzen, T. & Lindenberger, U. *PeerJ* **8**, e9290 (2020).
18. Franke, K. & Gaser, C. *GeroPsych: The Journal of Gerontopsychology and Geriatric Psychiatry* **25**, 235–245 (2012).
19. Gielen, M. et al. *Behav Genet* **38**, 44–54 (2008).
20. Kirkwood, T.B.L. *Cell* **120**, 437–447 (2005).
21. Shafto, M.A. et al. *BMC Neurol* **14**, (2014).
22. Taylor, J.R. et al. *NeuroImage* **144**, 262–269 (2017).
23. Bertram, L. et al. *Int J Epidemiol* **43**, 703–712 (2014).

24. Rajaram, S. et al. *Front Aging Neurosci* **8**, (2017).

25. Vidal-Piñeiro, D. et al. *Brain Stimul* **7**, 287–296 (2014).

26. Nilsson, L.-G. et al. *Aging, Neuropsychology, and Cognition* **11**, 134–148 (2004).

27. Ellis, K.A. et al. *Int Psychogeriatr* **21**, 672–687 (2009).

28. Reuter, M., Schmansky, N.J., Rosas, H.D. & Fischl, B. *NeuroImage* **61**, 1402–1418 (2012).

29. Dale, A.M., Fischl, B. & Sereno, M.I. *Neuroimage* **9**, 179–194 (1999).

30. Fischl, B., Sereno, M.I. & Dale, A.M. *Neuroimage* **9**, 195–207 (1999).

31. Fischl, B. & Dale, A.M. *Proc. Natl. Acad. Sci. U.S.A.* **97**, 11050–11055 (2000).

32. Walhovd, K.B. et al. *Proc. Natl. Acad. Sci. U.S.A.* **109**, 20089–20094 (2012).

33. Bycroft, C. et al. *Nature* **562**, 203–209 (2018).

34. Chang, C.C. et al. *Gigascience* **4**, 7 (2015).

35. Jonsson, B.A. et al. *Nature Communications* **10**, 5409 (2019).

36. Ge, T., Chen, C.-Y., Ni, Y., Feng, Y.-C.A. & Smoller, J.W. *Nature Communications* **10**, 1776 (2019).

37. International HapMap 3 Consortium et al. *Nature* **467**, 52–58 (2010).

38. Boyle, E.A., Li, Y.I. & Pritchard, J.K. *Cell* **169**, 1177–1186 (2017).

39. Lange, A.-M.G. de et al. *PNAS* **116**, 22341–22346 (2019).

40. Rogosa, D.R. & Willett, J.B. *Psychometrika* **50**, 203–228 (1985).

41. Wainer, H. *Psychol Sci* **11**, 434–436 (2000).

42. Nilsen, T.S., Kutschke, J., Brandt, I. & Harris, J.R. *Twin Res Hum Genet* **20**, 406–413 (2017).

43. Tehranifar, P., Liao, Y., Flom, J.D. & Terry, M.B. *Am J Epidemiol* **170**, 910–917 (2009).

44. Lakens, D., Scheel, A.M. & Isager, P.M. *Advances in Methods and Practices in Psychological Science* **1**, 259–269 (2018).